Oncogene (2003) 22, 1501–1510

www.nature.com/onc

PDGF-D is a potent transforming and angiogenic growth factor

Hong Li, Linda Fredriksson, Xuri Li and Ulf Eriksson

Ludwig Institute for Cancer Research, Stockholm Branch, Box 240, S-171 77 Stockholm, Sweden

Platelet-derived growth factors (PDGFs) are important for normal tissue growth and maintenance. Overexpression of the classical PDGFs, PDGF-A and PDGF-B, has been linked to several diseases, including cancer, fibrotic disease and atherosclerosis. Recently, two novel PDGFs, PDGF-C and PDGF-D, were discovered. It has not yet been established whether PDGF-C and PDGF-D are linked to disease phenotypes like the classical PDGFs. PDGF-B, the cellular homologue of the viral simian sarcoma oncogene v-*sis*, is known to potently induce cellular transformation through activation of PDGF receptor (PDGFR)-β. In this work, we have determined the transformation efficacy of PDGF-D in comparison with that of PDGF-C and PDGF-B. PDGF-D is a potent transforming growth factor for NIH/3T3 cells, and the transformed cells displayed stress fibre reorganization, increased proliferation rate, anchorage-independent growth in soft agar, ability to induce tumours in nude mice, and upregulation of vascular endothelial growth factor. Morphological analyses of the vasculatures from the PDGF-isoform-expressing tumours revealed marked differences suggesting differential signalling through the two PDGF receptors in tumour vessel development and remodelling. In summary, these results suggest that PDGF-D induce cellular transformation and promote tumour growth by accelerating the proliferation rate of the tumour cells, and by stimulation of tumour neovascularization.
Oncogene (2003) **22,** 1501–1510. doi:10.1038/sj.onc.1206223

Keywords: PDGF; VEGF; transformation; growth factor; tumour growth; angiogenesis

Introduction

Platelet-derived growth factors (PDGFs) regulate diverse cellular functions in connective tissue cells, and are important for normal embryonic development (Soriano, 1994; Boström *et al*., 1996; Lindahl *et al*., 1997). PDGFs exert their cellular effects by activating two structurally related receptor tyrosine kinases, PDGFR-α and PDGFR-β. Thus far, the PDGF family of growth factors consists of four members; the classical PDGF chains, PDGF-A and PDGF-B, which have been studied intensively, and the newly isolated PDGF-C (Li *et al*., 2000) and PDGF-D chains (Bergsten *et al*., 2001; LaRochelle *et al*., 2001). PDGF-C and PDGF-D have a two-domain organization unique within the PDGF family. Both factors possess an N-terminal domain, referred to as the CUB domain (*C*omplement subcomponents C1r/C1s, *U*rchin EGF-like protein and *B*one morphogenic protein-1) (Bork, 1991), in front of the conserved growth factor domain. The role of the CUB domain is currently unknown; however, proteolytic removal of the CUB domain is required before PDGF-C and PDGF-D can bind to and activate their cognate PDGFRs. In previous studies, we have shown that PDGF-C preferentially signals through PDGFR-α and PDGF-D through PDGFR-β. However, other groups have demonstrated that both PDGF-D and PDGF-C are able to activate PDGFR-α/β heterodimeric complexes as well (Gilbertson *et al*., 2001; LaRochelle *et al*., 2001).

PDGF-BB, which can bind and activate both PDGFR-α and PDGFR-β, has been shown to be a potent proto-oncogene that functions similar to the oncogene v-*sis* of simian sarcoma virus to transform fibroblastic NIH/3T3 cells (Gazit *et al*., 1984). Up-regulation and/or structure rearrangement of PDGFs and PDGFRs have been found in many tumours suggesting important roles in tumour growth (Fleming *et al*., 1992; Simon *et al*., 1997). In contrast to PDGF-BB, PDGF-AA fails to effectively transform fibroblastic cells, and since PDGF-AA signals exclusively through PDGFR-α, it has been suggested that the transformation activity of PDGF-BB is mediated through PDGFR-β signalling (Heldin and Westermark, 1999; Yu *et al*., 2000). Recently, PDGF-C was found to be an EWS/FLI-induced transforming growth factor (Zwerner and May, 2001). The transforming activity of PDGF-C might thus be explained by activation of PDGFR-β via binding to PDGFR-α/β heterodimeric complexes (Gilbertson *et al*., 2001). In addition, the expression of PDGF-C in many tumour cell lines further indicates a role of PDGF-C in tumorigenesis (Uutela *et al*., 2001).

PDGF-D has also been found to be expressed in many tumour cell lines; however, the biological role of PDGF-D in tumorigenesis remains elusive (Uutela *et al*., 2001; LaRochelle *et al*., 2002; Lokker *et al*., 2002). Since PDGF-D preferentially signals through PDGFR-β, we addressed the question whether PDGF-D could induce cellular transformation and support tumour development similar to PDGF-B. Thus, we stably transfected mouse full-length PDGF-D in NIH/3T3 cells as well as

*Correspondence: U Eriksson; E-mail ueri@licr.ki.se
Received 5 June 2002; revised 30 October 2002; accepted 6 November 2002

PDGF-B and PDGF-C for a comparison. The transfectants adopted a transformed morphology, with actin reorganization, increased proliferation and anchorage-independent growth, and with the ability to induce tumour formation in nude mice. The transformation of the NIH/3T3 cells by PDGF-D also induced VEGF expression. These results establish a role for PDGF-D in tumorigenesis and angiogenesis through both autocrine and paracrine stimulation.

Results

Overexpression of PDGF-D in NIH/3T3 cells downregulates both PDGFR-α and PDGFR -β expression and activation

To characterize the effect of PDGF-D in tumorigenesis, full-length mouse PDGF-D was expressed in NIH/3T3 cells. As positive controls, full-length PDGF-C, recently shown to be a transforming growth factor, and PDGF-B, a classical transforming growth factor, were also expressed in NIH/3T3 cells. Serum-free media from stable transfected PDGF-D and PDGF-C cells were collected and subjected to protein expression analysis. Expression of full length, but also processed forms of PDGF-D and PDGF-C were elevated in the growth factor transfectants as compared to the endogenous expression levels detected in cells transfected with empty vector (negative control) (Figure 1a, b). PDGF-B mRNA expression levels were verified by RT–PCR, and it was found that PDGF-B was exclusively expressed in the PDGF-B-transfected cells (data not shown).

The expression levels of PDGFR-α and PDGFR-β and their phosphorylation status in the stable transfectants and wild-type cells were compared. Immunoprecipitation with antibodies against PDGFR-α (Figure 1c) and PDGFR-β (Figure 1d) was followed by immunoblotting using monoclonal antiphosphotyrosine antibody to detect receptor phosphorylation, or polyclonal C-terminal receptor antibodies for the receptor expression levels. Both PDGFR-α and PDGFR-β expression and phosphorylation levels were downregulated in all growth factor-expressing cells as compared to wild-type and vector transfected cells (Figure 1c, d; left panels). To validate the experimental system, the various transfectants and wild-type cells were stimulated with recombinant PDGF-BB before immunoprecipitation using the same experimental settings (Figure 1c, d; right panels). As expected, PDGF-BB stimulation increased tyrosine phosphorylation of both PDGFR-α and PDGFR-β in wild-type and vector transfectants as compared to unstimulated cells. However, PDGF-BB treatment did not induce further activation of PDGFR-α and did only mildly increase phosphorylation of PDGFR-β in the growth factor transfectants (Figure 1c, d; right panel). In an attempt to understand the molecular mechanism underlying short-term *vs* long-term stimulation with PDGFs, wild-type cells were stimulated with PDGF-BB for different time course (Figure 1e). PDGFR-β was then immunoprecipitated and the phosphorylation status detected as described above. In contrast to short-term treatment, long-term stimulation nearly abolished the phosphorylation. However, no obvious change in receptor level was observed after 24 h of treatment. These results suggest that both PDGFRs are downregulated in NIH/3T3 cells constitutively over-expressing the growth factors.

PDGF-D induces actin reorganization, reduces cell-substrate focal contacts and promotes cell growth in NIH/3T3 cells

During cell culturing, the morphology of the stable PDGF-D transfectants changed into a smaller and more rounded-up shape as compared to wild-type and vector control cells, which resembled the morphology of the PDGF-B transfectants. PDGF-C transfectants had yet another appearance, as they were bigger and less rounded-up than both the PDGF-D- and PDGF-B-expressing cells. After each passage, the growth factor-expressing cells needed more time for attachment compared to controls. To confirm our observations, we stained the cells with rhodamine-labelled phalloidin to visualize F-actin filaments, and vinculin to detect cell-substrate focal contacts (Figure 2). The PDGF-D- and PDGF-B-expressing cells had lost their normal stress fibres and displayed circular actin structure, while the PDGF-C-expressing cells had decreased numbers of normal stress fibres as compared to controls (Figure 2, left panel). Considering the differential binding of PDGF-B, PDGF-C and PDGF-D to the two PDGFRs, it is not surprising that there is a morphological

Figure 1 Growth factor expression and receptor analysis in NIH/3T3 transfectants. **(a,b)** Secretion of PDGF-C and PDGF-D from transfected NIH/3T3 cells. Serum-free media were TCA precipitated and equal amounts of protein were subjected to SDS–PAGE under reducing conditions and then immunoblotted using antibodies against PDGF-C and PDGF-D, respectively. Full-length proteins and processed species were detected (arrow heads). Endogenous expression of both PDGF-C and PDGF-D was low in vector-transfected cells. **(c,d)** Expression and activation of PDGF receptors. Transfectants and wild-type cells were either unstimulated (left panels) or stimulated (right panels) by PDGF-BB (10 ng/ml) and then immunoprecipitated with PDGFR-α (c) or PDGFR-β (d) specific antisera. Immunoprecipitates were subjected to SDS–PAGE and immunoblotted using monoclonal antiphosphotyrosine antibody (PY99) to detect receptor phosphorylation (upper panel). The blots were stripped and reblotted with CED antiserum against the C-terminal of PDGFRs (middle panel) for the receptor expression levels. Both PDGFR-α and PDGFR-β expression and phosphorylation were downregulated in the growth factor transfectants as compared to vector controls and wild-type cells. IgG heavy chain was used as internal loading control (lower panel). **(e)** Determination of the phosphorylation status of PDGFR-β in NIH/3T3 cells upon short- and long-term stimulation by PDGF-BB. NIH/3T3 cells were starved overnight and then treated with PDGF-BB either on ice, or at 37°C for different time points. PDGFR-β was immunoprecipitated and the receptor phosphorylation detected as described above. PDGFR-β phosphorylation level was the highest after 1 h of stimulation and nearly vanished after 24 h

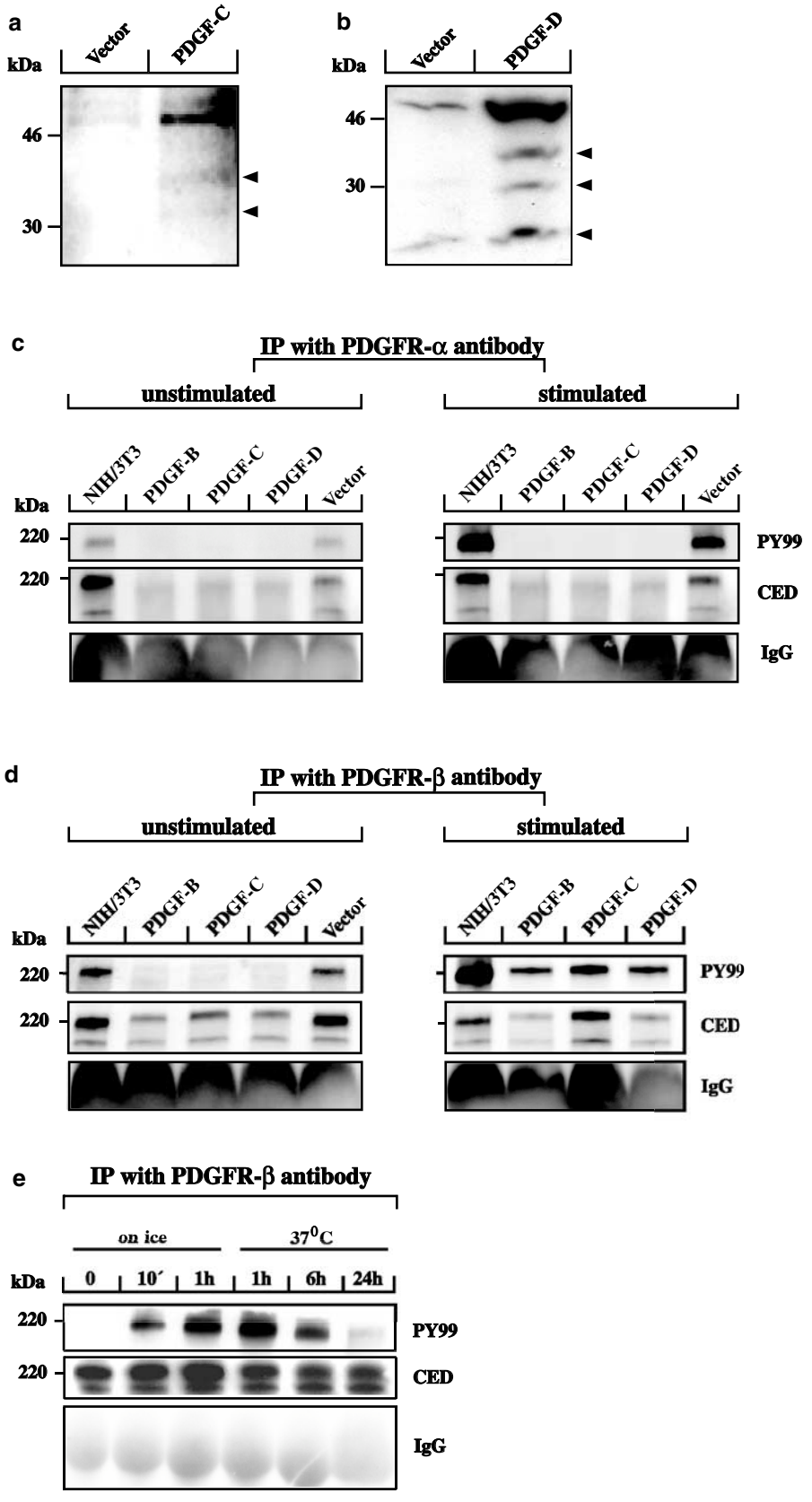
a
kDa
Vector
PDGF-C
46
30
b
kDa
Vector
PDGF-D
46
30
c
IP with PDGFR-α antibody
unstimulated
stimulated
NIH/3T3
PDGF-B
PDGF-C
PDGF-D
Vector
kDa
220
220
PY99
CED
IgG
d
IP with PDGFR-β antibody
unstimulated
stimulated
NIH/3T3
PDGF-B
PDGF-C
PDGF-D
Vector
kDa
220
220
PY99
CED
IgG
e
IP with PDGFR-β antibody
on ice
37°C
kDa
0
10′
1h
1h
6h
24h
220
220
PY99
CED
IgG

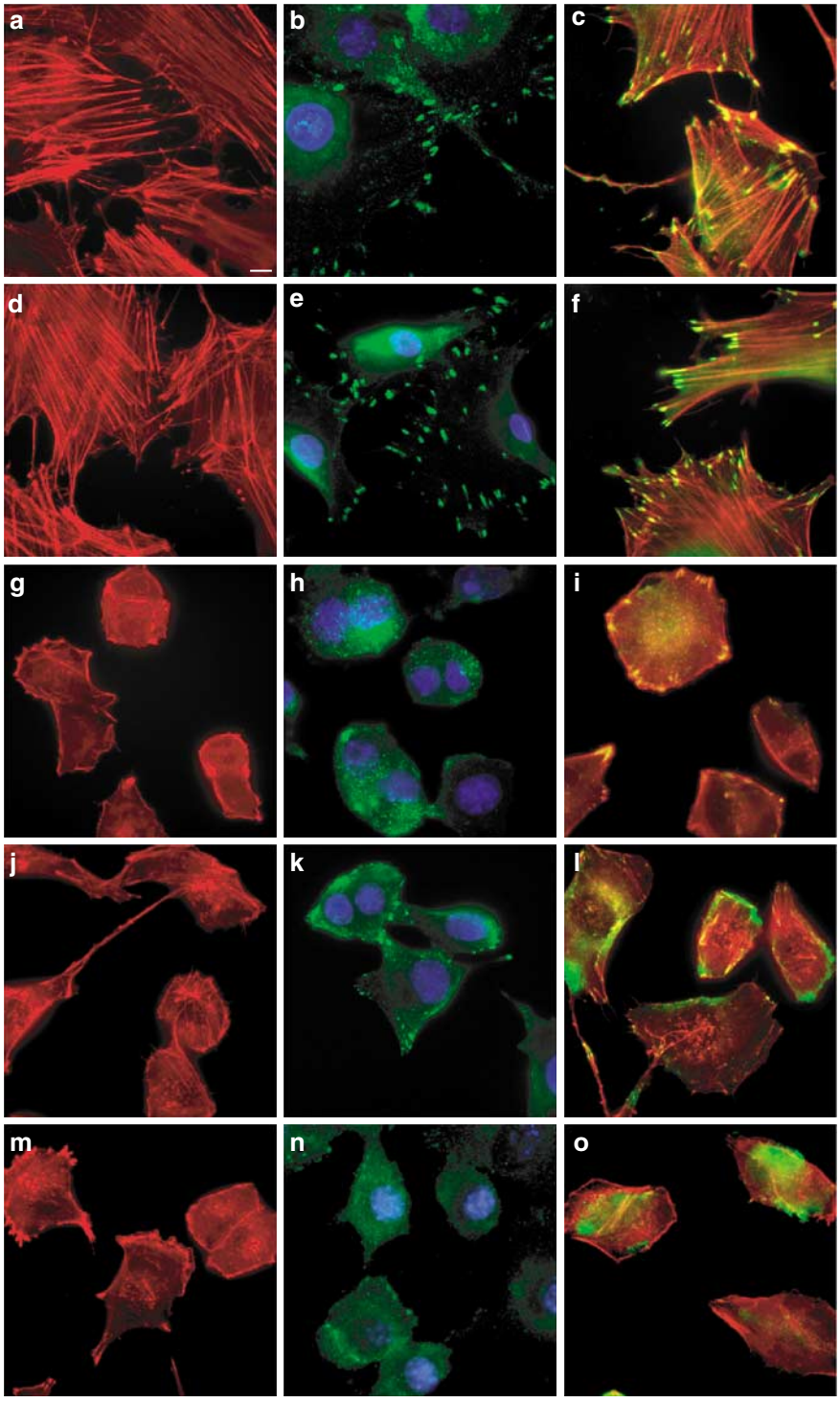

Figure 2 Actin reorganization and loss of vinculin-positive adhesion plaques in growth factor-transfected NIH/3T3 cells. Immunofluorescent staining was performed in **(a–c)** wild-type, **(d–f)** vector, **(g–i)** PDGF-B, **(j–l)** PDGF-C and **(m–o)** PDGF-D as described in Materials and methods. F-actin filaments were visualized with rhodamine-labelled phalloidin (left panel in red) and typical stress fibre organization was seen in wild-type and vector controls, whereas the growth factor-expressing cells had decreased numbers of stress fibres. Specific staining of vinculin (middle panel in green) at cell-substrate adhesion plaques was apparent in control cells, but was essentially lost in the growth factor transfectants. Nuclear counterstaining was achieved with DAPI (blue). Overlays for F-actin and vinculin staining displayed colocalization at cell-substrate focal contacts more prominent in wild-type and vector-transfected cells (right panel in yellow). Bar, 20 μm

difference between the growth factor-expressing cells. Whereas both PDGFRs promote edge ruffling and loss of stress fibres, only the PDGFR-β mediates the formation of circular actin structures on the dorsal surface of the cell (Eriksson *et al*., 1992). The cells were also stained with vinculin, a protein which links the actin cytoskeleton to the cell membrane at sites of cell-substrate focal contacts. Specific staining of vinculin at focal contacts was apparent in control cells, but was essentially lost in the growth factor transfectants (Figure 2, middle panel).

The proliferation rates of the transfected cells in either normal or serum-free culture conditions were evaluated. Under normal culture conditions using serum addition, the elevated expression of PDGF-D and PDGF-C led to a higher growth rate than in the vector transfectants, indicating these two growth factors can promote cell proliferation even in serum-containing medium (Figure 3a). Under serum-free conditions, PDGF-D- and PDGF-C-expressing cells kept proliferating, whereas the vector transfectants and wild-type cells underwent serum-deprivation-induced cell death (Figure 3b). These data suggest that PDGF-D and PDGF-C stimulation increase cell proliferation and cell survival. The ability to activate the full-length growth factors under serum-free condition suggests that the NIH/3T3 cells express the appropriate protease(s) to carry out this function. Since the steady-state level of PDGFR was decreased in the growth factor transfectants (Figure 1c, d), we hypothesized that the increase in proliferation rate in the PDGF-D and PDGF-C transfectants was because of activation of the downstream mitogenic signalling pathways. Therefore, the p42/p44 MAPK activity was analysed (Figure 3c). In all growth factor transfectants, there was an MAPK size shift, which is indicative of MAPK activation (Franke *et al*., 1995).

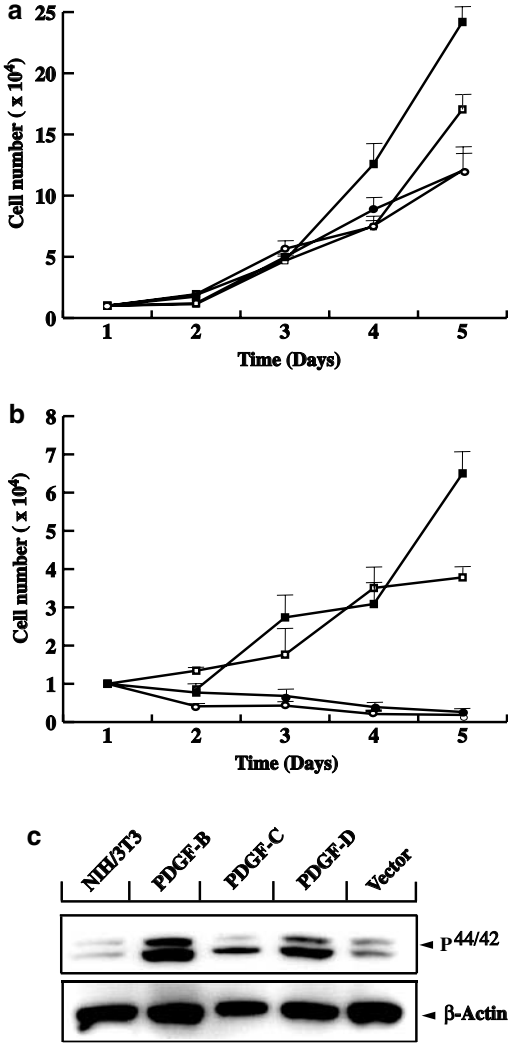

Figure 3 Growth of PDGF-C- and PDGF-D-expressing NIH/3T3 cells in normal and serum-free media and p44/42 activation in the growth factor transfectants. Cell growth analysis under **(a)** normal and **(b)** serum-free conditions showed that the growth factor transfectants, in contrast to controls, were able to grow in serum-free medium. The experiments were repeated twice and representative curves are shown. The values are means of triplicates $\pm$ s.d. (-□-, PDGF-D; -■-, PDGF-C; -●-, vector; -○-, wild type). **(c)** Wild-type and all the transfected cells were serum starved overnight, and equal amounts of cell lysates were subjected to Western blotting to detect p44/42 activation. There was a size shift from p44 to p42 in the growth factor transfectants, while in the wild-type and vector-transfected cells the two bands had equal intensity. β-Actin was used as a loading control

PDGF-D-expressing cells show anchorage-independent growth

To investigate whether PDGF-D could induce cellular transformation, we determined the ability of PDGF-D-expressing cells to grow as colonies in soft agar as compared to PDGF-B- and PDGF-C-expressing cells, wild-type cells and vector-transfected cells. The cells were plated in soft-agar-containing media at equal densities and after 3 weeks, formed foci were quantified (Figure 4). All the growth factor-expressing cells formed a large number of foci compared to controls with the highest amount of foci forming from PDGF-B-expressing cells. The foci morphology differed between the three PDGF-expressing cells, with larger foci forming from PDGF-D-expressing cells, smaller from PDGF-B cells and a mixture of both small and large foci forming from PDGF-C cells. It is possible that the observed differences in foci morphology are because of retention of PDGF-B to the cell surface causing it to act locally, whereas the other two PDGFs are more diffusible, thus affecting neighbouring cells as well. Based on these results, we concluded that PDGF-D is a potent transforming growth factor for NIH/3T3 cells.

PDGF-D induces tumour formation in nude mice

To test the ability of PDGF-D-expressing cells to induce tumour formation, cells were injected subcutaneously in the midline dorsum of Balb/C nude mice. As controls, PDGF-B-expressing, PDGF-C-expressing, and vector-transfected cells were included. All growth factor

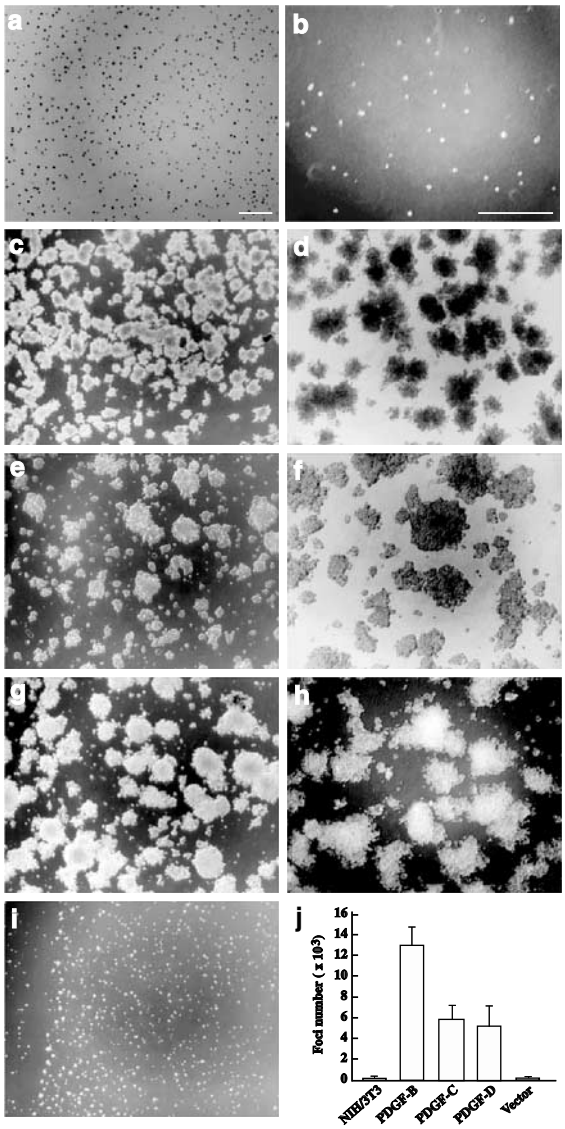

Figure 4 Anchorage-independent growth of PDGF-B-, PDGF-C- and PDGF-D-expressing NIH/3T3 cells in soft agar. **(a,b)** Wild-type, **(c,d)** PDGF-B, **(e,f)** PDGF-C, **(g,h)** PDGF-D and **(i)** vector-transfected NIH/3T3 cells were grown in soft agar as described in Material and methods. The microphotographs show representative areas of the plates at low (left panel) and high (right panel) magnification. The growth factor transfectants form foci, and the morphology of the foci differ between the PDGF-B-, PDGF-C- and PDGF-D-expressing cells. **(j)** Quantification of the number of foci. The experiment was repeated twice. The values are means of triplicates $\pm$ s.d. Bars, 0.5 mm

transfectants formed tumours. However, the PDGF-B- and PDGF-C-expressing cells formed tumours faster than PDGF-D-expressing cells (Figure 5a). No appreciable growth of the vector-transfected cells was seen.

It is well established that PDGFR-β activation by PDGF-BB or PDGF-AB induces VEGF-A mRNA expression through the PI3K or PKC pathways (Wang *et al*., 1999). We therefore investigated whether PDGF-D and PDGF-C, like PDGF-B, could induce VEGF expression, which might then promote tumour development indirectly by stimulation of tumour angiogenesis. Immunoblot analysis of secreted VEGF present in conditioned media showed increased levels in all growth factor transfectants as compared to vector control, with PDGF-C-expressing cells secreting the highest amount of VEGF (Figure 5b). These results were supported by VEGF transcript analysis by RNase protection analysis (RPA), which showed that VEGF mRNA was upregulated four times in PDGF-C-expressing cells and 1.5–1.7 times in PDGF-B and PDGF-D cells as compared to wild-type and vector-transfected cells (data not shown). Thus, *in vivo* tumorigenesis and angiogenesis initiated by PDGF-D, PDGF-C and PDGF-B may partially be explained by the induction of VEGF expression.

Vessel morphology in PDGF-isoform-expressing tumours

Histological analysis of the various PDGF-expressing tumours of similar size revealed the presence of the transformed NIH/3T3 cells and infiltrating fibroblasts from the host (Figure 5c). It appeared that there were more infiltrating fibroblasts in the PDGF-C-derived tumours. We examined the blood vessel phenotypes and the vascular densities in the tumours by staining sections with the endothelial cell marker, platelet/endothelial cell adhesion molecule (PECAM), and with a vascular smooth muscle cell marker, smooth muscle α-actin (SMA). PECAM staining of PDGF-D-expressing tumour tissue showed long and irregularly shaped vessels with a phenotype similar to PDGF-B-expressing tumour tissue (Figure 5d). The vascular pattern in PDGF-C-expressing tumour tissue was different, with more small and less large vessels as compared to PDGF-B- and PDGF-D-expressing tumours. The vessel densities and the size distributions of the stained vessels were quantified. The total number of vessels in the PDGF-D- and PDGF-C-expressing tumours was significantly higher compared to the PDGF-B-expressing tumour (PDGF-D *vs* PDGF-B, $P<0.006$ and PDGF-C *vs* PDGF-B, $P<0.009$) (Figure 5f). Given the different size distributions of the vessels in the different tumours, the counted vessels were subgrouped into three categories, defined as small (length $<10\,\mu$m), medium ($10\,\mu$m $>$ length $<30\,\mu$m) and large (length $>30\,\mu$m). The number of small vessels in PDGF-D-expressing tumours was increased by about 1.7-folds ($P<0.05$) and more than twofold ($P<0.001$) in PDGF-C tumours as compared to PDGF-B-expressing tumours. Comparison of PDGF-D to PDGF-C showed that the number of small vessels was significantly higher ($P<0.05$) in PDGF-C-expressing tumours. PDGF-D tumours had nearly the same density of large vessels as PDGF-B, whereas PDGF-C tumours had significantly fewer as compared to the PDGF-D- and PDGF-B- expressing tumours ($P<0.05$). SMA staining of the different growth factor-expressing tumours showed that there were more large SMA-positive vessels in the PDGF-D- and PDGF-B-derived tumours than in the PDGF-C tumours (Figure 5e). The total number of SMA-positive vessels was quantified and was significantly higher in the

PDGF-C ($P<0.05$)-derived tumours as compared to the PDGF-B-expressing tumours (Figure 5g).

Discussion

In this study, we have identified that exogenous expression of PDGF-D in NIH/3T3 cells induce cellular transformation indicated by the characteristic changes in cellular morphology caused by reorganization in the actin cytoskeleton, enhanced growth in serum-free medium, changes in adhesion properties and growth in soft agar, and *in vivo* tumorigenesis and angiogenesis. The transforming efficacy of PDGF-D was found to be similar to the known transforming growth factors PDGF-B and PDGF-C. Together with the observation that PDGF-D is expressed in many different types of tumour cell lines (Uutela *et al*., 2001; LaRochelle *et al*., 2002; Lokker *et al*., 2002), this suggests that PDGF-D may play a role in tumour development and progression, as the classical PDGFs have already been shown to do (Bronzert *et al*., 1987; Nister *et al*., 1991; Hsu *et al*., 1995).

Based on the preferential PDGFR-β specificity of PDGF-D, we predicted PDGF-D to function equally well as PDGF-B in transforming the fibroblastic NIH/3T3 cells, although the required proteolytic removal of the N-terminal CUB domain for receptor binding and activation added complexity to the prediction. However, the acquisition of processed forms of PDGF-D from full-length PDGF-D transfectants indicated that proteases capable of proteolytic activation of PDGF-D were expressed in NIH/3T3 cells. The observation that the foci formation and the tumour growth rates of the PDGF-D-expressing cells were reduced compared to that of the PDGF-B-expressing cells may, however, be an indication that the activation step for PDGF-D is rate limiting in this experimental system. Similarly, the NIH/3T3 cells were also able to activate PDGF-C.

Constitutive activation of PDGFRs by PDGF ligands leads to internalization and degradation of the receptors (Heldin and Westermark, 1999), possibly resulting in receptor downregulation and reduction in receptor phosphorylation as shown here. Despite the observed

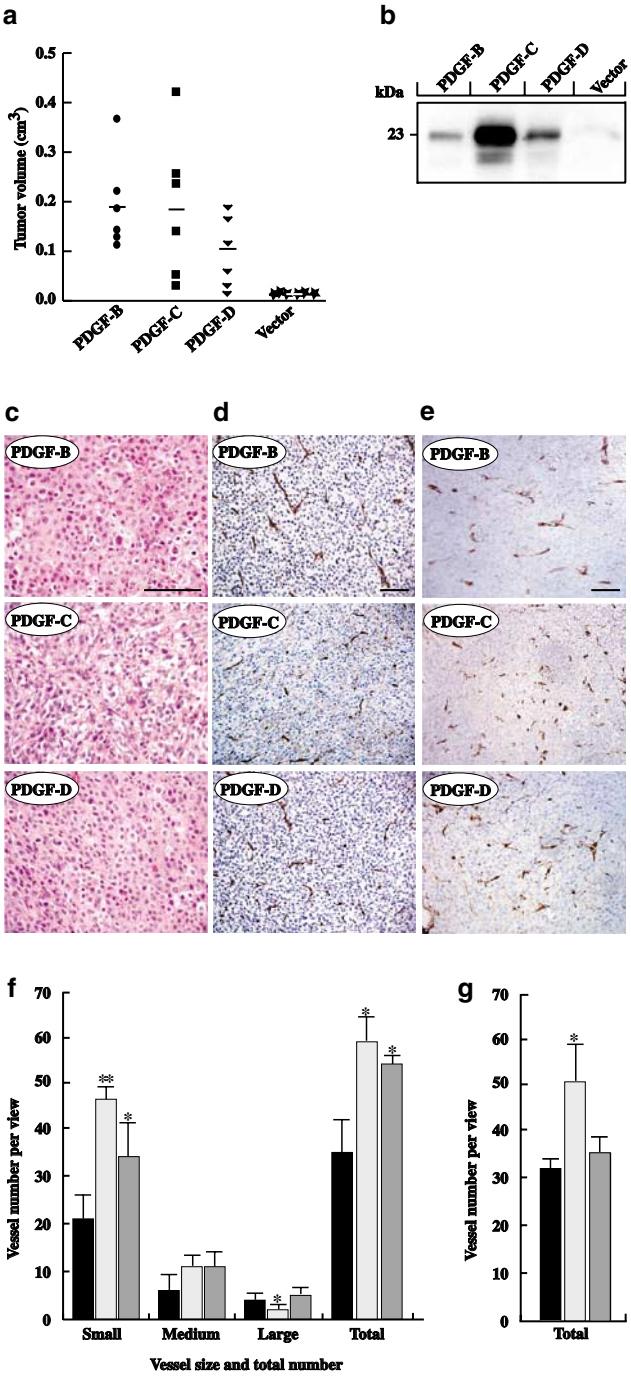

Figure 5 Tumour growth induced by PDGF-transfected NIH/3T3 cells injected into nude mice. In total, 1×10^6 growth factor and vector-transfected NIH/3T3 cells were injected subcutaneously into the midline dorsum of each mouse. **(a)** Tumour volumes 15 days after the injection of the PDGF-isoform-expressing cells. All growth factor transfectants induced tumour growth. The lines indicate the mean value of the tumour volumes. Tumour volumes were calculated as described in Materials and methods. **(b)** VEGF protein expression in growth factor-expressing cells and vector transfectants. The secreted VEGF protein levels were elevated in all the growth factor-expressing cells, with the highest amount detected in the PDGF-C-expressing cells. **(c)** Tumour tissues were stained with haematoxylin/eosin and all three PDGF-isoform-expressing tumours displayed a histology typical of fibrosarcomas with tumour cells mixed with invading host stroma. It appeared that more stromal cells were recruited in the PDGF-C-expressing tumours. **(d,e)** Immunohistochemical staining of PDGF-isoform-expressing tumours. The sections were stained with antibodies to (d) PECAM and (e) SMA. **(f,g)** Vessel numbers in the (f) PECAM- and (g) SMA-stained tumour tissue sections. A total of 10 randomly selected views per section were analysed, and the stained vessels were counted. In the PECAM-stained sections, vessels larger than 30 μm were considered as large, larger than 10 μm but less than 30 μm as medium, and vessels less than 10 μm in diameter as small. In the SMA-stained sections, only the total vessel numbers were counted. The vessel numbers are the mean values from each group $\pm$ s.d. PDGF-C- and PDGF-D-expressing tumours had significantly more small vessels than PDGF-B-expressing tumours and also, PDGF-C-expressing tumours had fewer large vessels than both PDGF-D- and PDGF-B-expressing tumours. PDGF-B, black bar; PDGF-C, light grey bar; PDGF-D, dark grey. Six tumours from each variant were sectioned and analysed. Scale bars, 50 μm

reduction in receptor phosphorylation in the growth factor transfectants, the downstream mitogenic signalling pathway was being activated causing the higher proliferation of these cells compared to controls. It is however noteworthy that PDGF-D-transfected cells had similar receptor expression and phosphorylation status as both PDGF-B and PDGF-C transfectants considering their respective receptor binding preferences. This might be explained by the activation of both the PDGFRs via binding of PDGF-D, and also PDGF-C, to PDGFR-α/β heterodimeric complexes.

Previous work has identified the PDGFs as potent angiogenic factors. In a chick chorioallantoic membrane (CAM) assay, PDGF-BB was found to induce consistently an angiogenic response whereas PDGF-AA was less active, and that this induction was direct through activation of embryonic chorioallantoic endothelial cell proliferation (Risau *et al*., 1992). In an *in vitro* assay for cord/tube formation of bovine aortic endothelial cells, PDGF-BB could increase tube formation via PDGFR-β, while PDGF-AA had no effect (Battegay *et al*., 1994). Using the corneal pocket assay, we have recently found that the recombinant form of activated PDGF-CC had the same ability to induce new vessel formation as PDGF-BB, whereas PDGF-AA was less effective (Cao *et al*., 2002). The mechanisms of action underlying the angiogenic properties of the PDGFs remain poorly characterized, but it has been suggested that PDGFR-β activation by PDGF-BB or PDGF-AB induce VEGF-A mRNA expression through the PI3K or PKC pathways (Wang *et al*., 1999). At least in part, this mechanism may underlie our observation that the PDGF-D and PDGF-C, like PDGF-B, transfectants upregulate VEGF expression.

It is well known that tumour angiogenesis leads to the formation of a poorly organized, and constantly remodelling vasculature with tortuous and leaky vessels with irregular vessel diameters (Jain, 1988; Hashizume *et al*., 2000). The failure of tumour vessels to properly recruite perivascular cells (vascular smooth muscle cells and pericytes) to stabilize the vessels is thought to contribute to the abnormal phenotype of tumour vessels (Abramsson *et al*., 2002). As PDGFs are known to be potent mitogens for perivascular cells, and affect their migration, we studied the structure of the tumour vasculature by staining tumour sections for PECAM and SMA expression to reveal possible differences. Interestingly, the vascular phenotypes were similar in PDGF-B- and PDGF-D-expressing tumours, while the vessels in the PDGF-C-expressing tumour were different. Quantification revealed that the PDGF-C-expressing tumours had increased number of small vessels ($<10\,\mu$m) compared to PDGF-D and PDGF-B-expressing tumours, possibly because of more secreted VEGF protein. On the other hand, PDGF-D and PDGF-B tumours gave rise to more larger vessels with variable vessel diameters. These observations are consistent with the receptor preferences for the PDGFs, suggesting that signalling through PDGFR-α and PDGFR-β have distinct effects on the growing tumour vasculature. Thus, PDGFR-α signalling appears to promote the formation of a vasculature with increased numbers of capillaries, while PDGFR-β signalling promotes a phenotype with more large vessels.

It is well established that different human tumours display heterogenous angiogenesis and blood vessel phenotypes (Eberhard *et al*., 2000), and in part this may be explained by differential expression of various growth factors for the different cell types of the vascular wall. An interesting future aspect of our work will consequently be to elucidate the cellular compositions of the vessels in the different PDGF-expressing tumours to gain further understanding of the role of the various PDGFs in the tumour vessel growth, perivascular cell recruitment and vessel remodelling.

During the preparation of this manuscript, LaRochelle *et al*. (2002) reported that the truncated form of PDGF-D was able to transform NIH/3T3 by analysing the growth rates of tumours from such cells in immunocompromised mice, whereas other important aspects of the transformed phenotype was not reported. These authors also reported that NIH/3T3 cells expressing the full-length version of PDGF-D failed to transform, a result contradicting the present work. Clonal variations in the ability to process and activate the full-length protein may be the underlying reason, thus reinforcing the importance of further knowledge concerning the nature and mechanisms of action of the involved proteases.

Materials and methods

Plasmid constructs, cell culture and transfection

Mouse full-length PDGF-D and PDGF-C, and human PDGF-B cDNAs were cloned into pcDNA3.1/zeo(+) mammalian expression vector (Invitrogen). The nucleotide sequence and orientation of all the expression constructs were verified by sequencing.

NIH/3T3 cells were maintained in Dulbecco's modified Eagle medium (DMEM) supplemented with 10% fetal calf serum (FCS), 2 mM glutamine, 100 U/ml penicillin, and 100 μg/ml streptomycin. The cells were cultured at 37°C in a humidified 5% CO_2 atmosphere. Plasmid DNA (5 μg) was transfected into semiconfluent cells in Petri dishes using Lipofectamine plus reagent (Life Technology). Stable transfectants were selected in culture media containing 700 μg/ml Zeocin (Invitrogen) for 3 weeks, and the resistant colonies were maintained in normal medium supplemented with 300 μg/ml Zeocin until use.

To monitor cell growth, cells transfected with PDGF-D, PDGF-C and vector, respectively, were seeded into 12-well plates at a density of 1×10^4 cells/well. For cells growing under serum-free conditions, medium was changed after attachment. The day after seeding, cells were trypsinized and counted everyday for 4 days using a Coulter counter. All the samples were in triplicates and the experiment was repeated twice.

Immunoblotting, receptor and transcript analysis

Wild-type and stable transfected NIH/3T3 cells (2×10^6 cells/75 cm^2 flask) were cultured in serum-free medium overnight. Media were collected and protein concentration determined (Bradford, 1976). In total, 35 μg protein was precipitated using

ice-cold 10% trichloroacetic acid (TCA). Precipitated proteins were washed several times with 80% ethanol and then subjected to SDS–PAGE using 12% polyacrylamide gels (BioRad) under reducing conditions. PDGF-C was detected by immunoblotting using affinity-purified polyclonal rabbit antibodies against PDGF-C (Li *et al*., 2000), and PDGF-D was detected using affinity-purified polyclonal antibody against a synthetic peptide corresponding to the murine PDGF-D amino-acid sequence (Bergsten *et al*., 2001). Bound antibodies were observed using Enhanced Chemiluminiscence Plus reagent (ECL+, Amersham). To determine the activation of p44/42 MAP kinase, wild-type and growth factor-transfected cells were serum starved overnight, and cell lysates subjected to 12% SDS–PAGE under reducing conditon. The p44/42 antigen was detected by the polyclonal antibody against a synthetic peptide derived from the sequence of rat p42 (Cell Signalling, #9102). For loading control, the same membrane was stripped in 62.5 mM Tris-HCl pH 6.7, 2% SDS and 100 mM 2-mercaptoethanol for 30 min at 55°C and reprobed with mouse β-actin (Amersham, N350). To detect secreted VEGF protein, the growth factor-transfected cells and vector controls were plated at similar densities, serum starved, and treated with 10 μg/ml heparin overnight. Equal volumes of the conditioned media were precipitated and 35 μg protein subjected to SDS–PAGE. VEGF protein was detected by anti-mouse VEGF antibody (R&D, YU08).

To monitor tyrosine phosphorylation of PDGFR-α and PDGFR-β, 2×10^6 wild-type and transfected NIH/3T3 cells were seeded on 90 mm Petri dishes. The cells were incubated for 60 min on ice in PBS supplemented with 1 mg/ml BSA in the absence or presence of 10 ng/ml PDGF-BB. Cells were lysed in 20 mM Tris-HCl pH 7.5, 0.5% Triton X-100, 0.5% desoxycholic acid, 150 mM NaCl, 5 mM EDTA, 200 μM orthovanadate and complete protease inhibitor cocktail. PDGFRs were immunoprecipitated using specific antisera (Eriksson et al., 1992). Precipitated proteins were separated by SDS–PAGE using 7.5% polyacrylamide gels under reducing conditions. Tyrosine phosphorylated receptors were detected by immunoblotting using an antiphosphotyrosine antibody (PY99, Santa Cruz) and bound antibodies were visualized as above. The membranes were stripped and reprobed using a polyclonal antibody against the C-terminal of the PDGFRs (CED) to detect receptor expression levels. Bound antibodies were visualized as above. To determine the phosphorylation status of PDGFR-β in NIH/3T3 cells upon short- and long-term stimulation, 1×10^6 cells were seeded and serum starved overnight. The cells were then either stimulated with PDGF-BB (10 ng/ml) on ice, or PDGF-BB was added in the serum-free media at 37°C for the times indicated. After the treatment, the cells were collected and lysed as above. PDGFR-β was immunoprecipitated and the phosphorylation detected as described.

Total cellular RNA was prepared using the guanidinium thiocyanate/acid phenol method and stored in −80°C. For the analysis of PDGF-B expression, RT–PCR was performed using oligo-dT primed single-strand cDNA, using gene-specific primers: 5′-GCTCCTTTGATGATCTCCAA (forward) and 5′-CAATCTCGATCTTTCTCACC (reverse). The 360 bp amplified product was analysed by agarose gel electrophoresis. RPA was performed according to the manufacturer's protocol (Ambion). Riboprobes were prepared using RNA polymerase (Promega) and ^{32}P-UTP (Amersham). A mouse cDNA fragment was used for making the VEGF probe resulting in two protected fragments of 495 and 345 bp corresponding to $VEGF_{164}$, and all other isoforms, respectively. Mouse GAPDH cDNA (Ambion, 7431), which generates a 316 bp protected fragment, was used as an internal control for quantification.

Immunofluorescence

Wild-type and transfected NIH/3T3 cells were seeded in six-well dishes on sterilized coverslips at a density of 5×10^4 cells/well. After 24 h, the cells were fixed in 4% paraformaldehyde (PFA) in PBS for 15 min at room temperature. Fixed cells were quenched in 10 mM glycin to remove residual PFA and then permeabilized using 0.1% Triton X-100 for 30 min at room temperature. Following permeabilization, F-actin was visualized by staining with 1.5 U/ml rhodamine-labelled phalloidin (Molecular Probes). Vinculin was localized by monoclonal antivinculin (1 : 100 dilution, Sigma) and visualized by FITC-conjugated secondary antibody (Sigma, F-0257). To visualize all nuclei, 4′,6-diamidine-2′-phenylindole dihydrochloride (DAPI 1 μg/ml, Roche) was included in the secondary antibody solution. Staining was viewed using a Zeiss Axiophot microscope.

Anchorage-independent growth of PDGF transfectants in soft agar

A 0.6% (w/v) bottom layer of low melting point agarose in normal medium was prepared in Petri dishes (90 mm). On top, a layer of 0.3% agarose containing 1×10^6 stable transfected cells were placed. The cells were fed twice a week with 1 ml of normal medium. After 3 weeks, foci were counted and photographed using a Nikon Eclipse TE 300 inverted microscope.

Tumour growth in nude mice and immunohistochemical stainings

For *in vivo* tumour growth, 8-week-old female Balb/C nude mice were anaesthetized by methoxyflurane and 1×10^6 exponentially growing transfectants or wild-type cells, suspended in 100 μl of PBS, were implanted subcutaneously in the midline dorsum of each mouse. Tumours were measured and excised when the tumour developed to 1 cm in diameter. Tumour volume was calculated using the following formula: $\text{width}^2 \times \text{length} \times 0.52$ (Boehm *et al*., 1997). Tumour tissues were fixed in 4% PFA in PBS, paraffin embedded, sectioned (6 μm), and stained with haematoxylin/eosin. Immunohistochemistry of sections was performed using antibodies directed against PECAM-1/CD31 (DAKO, M0823) and SMA (DAKO, M0853) according to the manufacturer's instructions. For vessel counting, slides stained for PECAM expression were viewed using a Nikon Eclipse E1000 microscope. Vessels were counted in 10 randomly selected high-magnification views per slide. Vessels at any direction with a length more than 30 μm were considered as large, more than 10 μm but less than 30 μm considered as medium, and less than 10 μm as small vessels. *P*-values were determined by using a two-tailed *t*-test assuming unequal variance with $P < 0.05$ considered significant. Data presented are mean ± s.d.

Acknowledgements
We thank Barbara Åkerblom for expert technical assistance and Kristian Pietras and Arne Östman for kindly providing us with PDGF-BB protein and PDGF receptor antibodies. This study was supported by the Swedish Research Council, the Novo Nordisk Foundation, and Karolinska Institutet.

References

Abramsson A, Berlin O, Papayan H, Paulin D, Shani M and Betsholtz C. (2002). *Circulation*, **105,** 112–117.

Battegay EJ, Rupp J, Iruela-Arispe L, Sage EH and Pech M. (1994). *J. Cell Biol.*, **125,** 917–928.

Bergsten E, Uutela M, Li X, Pietras K, Östman A, Heldin C-H, Alitalo K and Eriksson U. (2001). *Nat. Cell Biol.*, **3,** 512–516.

Boehm T, Folkman J, Browder T and O'Reilly MS. (1997). *Nature*, **390,** 404–407.

Bork P. (1991). *FEBS Lett.*, **282,** 9–12.

Boström H, Willetts K, Pekny M, Leveen P, Lindahl P, Hedstrand H, Pekna M, Hellström M, Gebre-Medhin S, Schalling M, Nilsson M, Kurland S, Tornell J, Heath JK and Betsholtz C. (1996). *Cell*, **85,** 863–873.

Bradford M. (1976). *Anal. Biochem.*, **72,** 248–254.

Bronzert DA, Pantazis P, Antoniades HN, Kasid A, Davidson N, Dickson RB and Lippman ME. (1987). *Proc. Natl. Acad. Sci. USA*, **84,** 5763–5767.

Cao R, Bråkenhielm E, Li X, Pietras K, Widenfalk J, Östman A, Eriksson U and Cao Y. (2002). *FASEB J.*, **16,** 1575–1583.

Eberhard A, Kahlert S, Goede V, Hemmerlein B, Plate KH and Augustin HG. (2000). *Cancer Res.*, **60,** 1388–1393.

Eriksson A, Siegbahn A, Westermark B, Heldin C-H, and Claesson-Welsh L. (1992). *EMBO J.*, **11,** 543–550.

Franke TF, Yang SI, Chan TO, Datta K, Kazlauskas A, Morrison DK, Kaplan DR and Tsichlis PN. (1995). *Cell*, **81**(5), 727–736.

Fleming TP, Saxena A, Clark WC, Robertson JT, Oldfield EH, Aaronson SA and Ali IU. (1992). *Cancer Res.*, **52,** 4550–4553.

Gazit A, Igarashi H, Chiu IM, Srinivasan A, Yaniv A, Tronick SR, Robbins KC and Aaronson SA. (1984). *Cell*, **39,** 89–97.

Gilbertson DG, Duff ME, West JW, Kelly JD, Sheppard PO, Hofstrand PD, Gao Z, Shoemaker K, Bukowski TR, Moore M, Feldhaus AL, Humes JM, Palmer TE and Hart CE. (2001). *J. Biol. Chem.*, **276,** 27406–27414.

Hashizume H, Baluk P, Morikawa S, McLean JW, Thurston G, Roberge S, Jain RK and McDonald DM. (2000). *Am. J. Pathol.*, **156,** 1363–1380.

Heldin CH and Westermark B. (1999). *Physiol. Rev.*, **79,** 1283–1316.

Hsu S, Huang F and Friedman E. (1995). *J. Cell. Physiol.*, **165,** 239–245.

Jain RK. (1988). *Cancer Res.*, **48,** 2641–2658.

LaRochelle WJ, Jeffers M, Corvalan JR, Jia XC, Feng X, Vanegas S, Vickroy JD, Yang XD, Chen F, Gazit G, Mayotte J, Macaluso J, Rittman B, Wu F, Dhanabal M, Herrmann J and Lichenstein HS. (2002). *Cancer Res.*, **62,** 2468–2473.

LaRochelle WJ, Jeffers M, McDonald WF, Chillakuru RA, Giese NA, Lokker NA, Sullivan C, Boldog FL, Yang M, Vernet C, Burgess CE, Fernandes E, Deegler LL, Rittman B, Shimkets J, Shimkets RA, Rothberg JM and Lichenstein HS. (2001). *Nat. Cell. Biol.*, **3,** 517–521.

Li X, Pontén A, Aase K, Karlsson L, Abramsson A, Uutela M, Backström G, Hellström M, Boström H, Li H, Soriano P, Betsholtz C, Heldin CH, Alitalo K, Östman A and Eriksson U. (2000). *Nat. Cell. Biol.*, **2,** 302–309.

Lindahl P, Johansson BR, Leveen P and Betsholtz C. (1997). *Science*, **277,** 242–245.

Lokker NA, Sullivan CM, Hollenbach SJ, Israel MA and Giese NA. (2002). *Cancer Res.*, **62,** 3729–3735.

Nister M, Claesson-Welsh L, Eriksson A, Heldin CH and Westermark B. (1991). *J. Biol. Chem.*, **266,** 16755–16763.

Risau W, Drexler H, Mironov V, Smits A, Siegbahn A, Funa K and Heldin CH. (1992). *Growth Factors*, **7,** 261–266.

Simon MP, Pedeutour F, Sirvent N, Grosgeorge J, Minoletti F, Coindre JM, Terrier-Lacombe MJ, Mandahl N, Craver RD, Blin N, Sozzi G, Turc-Carel C, O'Brien KP, Kedra D, Fransson I, Guilbaud C and Dumanski JP. (1997). *Nat. Genet.*, **15,** 95–98.

Soriano P. (1994). *Genes Dev.*, **8,** 1888–1896.

Uutela M, Lauren J, Bergsten E, Li X, Horelli-Kuitunen N, Eriksson U and Alitalo K. (2001). *Circulation*, **103,** 2242–2247.

Wang D, Huang HJ, Kazlauskas A and Cavenee WK. (1999). *Cancer Res.*, **59,** 1464–1472.

Yu J, Deuel TF and Kim HR. (2000). *J. Biol. Chem.*, **275,** 19076–19082.

Zwerner JP and May WA. (2001). *Oncogene*, **20,** 626–633.